Nanoscale Res Lett (2008) 3:109–117
DOI 10.1007/s11671-008-9121-9

NANO EXPRESS

Grafting of Poly(methyl methacrylate) Brushes from Magnetite Nanoparticles Using a Phosphonic Acid Based Initiator by Ambient Temperature Atom Transfer Radical Polymerization (ATATRP)

Kothandapani Babu · Raghavachari Dhamodharan

Received: 20 November 2007 / Accepted: 14 February 2008 / Published online: 4 March 2008

Abstract Poly(methyl methacrylate) in the brush form is grown from the surface of magnetite nanoparticles by ambient temperature atom transfer radical polymerization (ATATRP) using a phosphonic acid based initiator. The surface initiator was prepared by the reaction of ethylene glycol with 2-bromoisobutyrl bromide, followed by the reaction with phosphorus oxychloride and hydrolysis. This initiator is anchored to magnetite nanoparticles via physisorption. The ATATRP of methyl methacrylate was carried out in the presence of CuBr/PMDETA complex, without a sacrificial initiator, and the grafting density is found to be as high as 0.90 molecules/nm^2. The organic–inorganic hybrid material thus prepared shows exceptional stability in organic solvents unlike unfunctionalized magnetite nanoparticles which tend to flocculate. The polymer brushes of various number average molecular weights were prepared and the molecular weight was determined using size exclusion chromatography, after degrafting the polymer from the magnetite core. Thermogravimetric analysis, X-ray photoelectron spectra and diffused reflection FT-IR were used to confirm the grafting reaction.

Keywords Magnetite nanoparticles · Organic–inorganic hybrid material · Phosphonic acid initiator · ATRP · Stable dispersion

Introduction

Magnetite (Fe_3O_4) exhibits cubic inverse spinal structure and is ferromagnetic below 860 K. The large oxygen ions are close packed in a cubic arrangement, while the smaller Fe ions fill in the gaps consisting of octahedral as well as tetrahedral sites. In the case of magnetite nanoparticles (MNs) the magnetic properties display wide varieties of interesting properties in contrast to the bulk [1]. MNs are well known for their potential applications in many diverse fields, such as magnetic ferrofluids [2], contrast agents for magnetic resonance imaging [3], biomedical application [4] and for drug delivery [5]. MNs tend to aggregate due to very strong magnetic dipole–dipole attraction. A polymeric stabilizer, grafted on to their surface, is required to prevent nanoparticle agglomeration so that a good dispersion can be achieved in various organic solvents [3]. A good dispersion in an organic solvent in turn would enable the use of lesser weight percent of filler for the same property enhancement.

The use of carboxylic acid based stabilizer, especially oleic acid based, [6] for anchoring to MNs followed by polymerization was reported. This is likely to provide less stable dispersions as the interaction between the carboxylic acid and magnetite is relatively weak with the binding being reversible, when compared with phosphonic acid/phosphonate groups, which form a stronger bond [7]. In order to introduce stronger bonding with the MNs surface, the chlorosilane anchoring moiety [8] was introduced in one step, followed by suitable polymerization. In this case, the liberated HCl (by the reaction of Si–Cl with surface –OH groups) can corrode the surface of the magnetite particles to form the less stable M–O–Si bond [9]. In another reported method [10] of nanoparticle stabilization, the silane moiety is anchored first, which is followed by a second step involving the reaction with the ATRP initiator, which is a heterogeneous reaction. This is then followed by polymerization.

Polymers can be anchored to nanoparticles by, (1) physisorption [11]—a weak force involving a weak bond

K. Babu · R. Dhamodharan (✉)
Department of Chemistry, Indian Institute of Technology—Madras, Chennai 600 036, India
e-mail: damo@iitm.ac.in

that is formed between the particle surface and the polymer segments; (2) grating to [7, 12] technique—the polymer end-group remains active and reacts with particle surface resulting in low grafting density; and (3) grafting from [13] technique defined as the growth of the polymer chains from one end of the chain initiator anchored to the particle surface through chemisorption (involves chemical bond formation and high grafting density by which the tethered polymer chains are forced to stretch away from the surface). Living radical polymerization techniques have been used to synthesize polymer brushes. These include nitroxide-mediated free radical polymerization [14], atom transfer radical polymerization (ATRP) [15] and reversible addition-fragmentation chain transfer (RAFT) [16].

Recently, phosphonate moiety was introduced, as an effective anchoring agent. The $-PO(OH)_2$ groups are known for their ability to complex metal ions that are stable even at elevated temperature, making them attractive for use in a variety of industrial applications. Phosphonates have a strong tendency to adsorb onto a variety of metal oxide surfaces such as Y_2O_3 [17], SnO_2 [18], Ta_2O_3 [19], zirconia and titania [20] and aluminium oxides [21] possibly through the formation of phosphonic acid ester, (by the reaction of surface –OH groups with the phosphonic acid although hydrogen bonding could be a stronger reason) resulting in the formation of metal–phosphonate (M–O–P) bonds. The phosphonic acid moiety can bind covalently with Fe^{+3} in the octahedral sites of MNs, and thus enable the retention of the magnetic property of the magnetite nanoparticle [22].

The use of phosphonic acid moiety for the surface anchoring, followed by polymerization on magnetite by nitroxide-mediated polymerization [23] was performed at a very high temperature, which favours thermal polymerization. In contrast, ATATRP [24] is less prone to side reaction as well as chain transfer. Further ATRP is a versatile technique [25] in which relatively low radical concentration in the reaction system is maintained to obtain narrow polydispersed polymer with a wide variety of tailored materials.

Based on the available literature it is essential to develop a one-step direct anchoring of initiator moiety, preferably phosphonic acid based, to magnetite surface that would enable the preparation of MNs with higher grafting density of the initiator groups and therefore could lead to higher grafting density of polymers (if the initiation takes place from all the initiator moieties anchored). In this work, an ATRP initiator is immobilized on to the magnetite nanoparticle surface in one step. The initiator containing an active tertiary bromide and a phosphonic end group is synthesized for this purpose. The poly(methyl methacrylate) is grown from the initiator covered MNs by copper-mediated atom transfer radical polymerization at ambient temperature. The polymer-encapsulated magnetite particles are then characterized.

Experimental Section

Materials

Methyl methacrylate (MMA) (Lancaster) was purified using a basic alumina column (to remove inhibitor), followed by deoxygenation by bubbling argon gas through the solution ~1 h) and stored under argon in the freezer (−10 °C). Ferrous sulphate (Lancaster), ferric chloride (Lancaster), ammonium hydroxide (Lancaster), 2-bromoisobutyryl bromide (Lancaster), copper(I)bromide (Aldrich,99.98%), *N*,*N*,*N*′,*N*″,*N*″-pentamethyldiethyl triamine (Aldrich, 99%), aluminium oxide (activated, basic, for column chromatography, 50–200 μm), and phosphorus oxychloride (SRL India) were used without purification. Triethylamine, anisole and ethylene glycol (SRL India) were used as received.

Synthesis of Magnetite Nanoparticle

A solution of ferrous and ferric ions in the molar ratio 1:2 was prepared by dissolving 1.76 g of ferrous sulphate (6.22 mmol) and 2.04 g of anhydrous ferric chloride (12.44 mmol) in a 50 mL aqueous solution, followed by sonication for 1 h at 25 °C. Magnetite was precipitated by adding the above mentioned mixed solution to a 200 mL aqueous solution of ammonia maintained at a pH ~ 10, in an inert atmosphere. The mixture was subsequently stirred for 30 min. After the precipitation, it was rinsed with deionized water several times and then separated by centrifugation at 10,000 rpm. It was dried under vacuum, at 50 °C for 24 h.

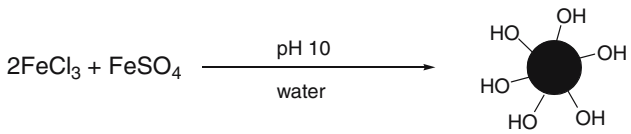

Synthesis of 2-bromo-2-methyl-propionic acid 2-hydroxy-ethyl ester [26]

Anhydrous ethylene glycol (110 mL, 2 mol), (a), was purged with argon gas in a 100-mL RB flask. Then, 2-bromoisobutyrl bromide (10 mL, 81 mmol) was added drop wise to the stirring solution, maintained at 0 °C, and it was allowed to stir for a further period of 3 h. It was then diluted with 50 mL of water and extracted with chloroform (3 × 100 mL). The organic extract was dried with anhydrous sodium sulphate, filtered and the filtrate was evaporated to dryness to yield slightly viscous and

colourless liquid, (b). It was characterized by FTIR and NMR. FTIR (ν cm^{-1}, film): broad absorption at ~3,400 (free aliphatic –OH group), 2,976 (aliphatic –CH), very sharp absorption at 1,731 (ester carbonyl –C=O). ^{1}H NMR (400 MHz, δ in ppm, $CDCl_3$): 4.29 (t, 2H, J = 4.8 Hz), 3.86 (t, 2H, J = 4.8 Hz), 3.05(s, 1H), 1.95 (s, 6H); ^{13}C NMR (400 MHz, δ in ppm, $CDCl_3$): 171.42, 67.26, 60.33, 55.88, 30.79.

Synthesis of 2-bromo-2-methyl-propionic acid 2-phosphonooxy-ethyl ester

Ethyl ester, (5.2 mL 33.83 mmol) (b), was dissolved in 90 mL of anhydrous THF and purged with argon.3.5 mL (37.23 mmol) of $POCl_3$ was added drop wise to this solution, which was maintained at 0 °C for 1h. It was further stirred for 3 h at ambient temperature. At the end of the reaction, it was then diluted with 60 mL of water and extracted with chloroform (3 × 100 mL). The organic extract was dried with anhydrous sodium sulphate, filtered and the filtrate was evaporated to dryness to yield viscous and yellow liquid, (c). FTIR (ν cm^{-1}, film): 2,976 (aliphatic –CH), 2,360 broad peak (phosphonic acid P–O–H), sharp absorption at 1,734 (ester carbonyl C=O), 1,273 (phosphonates P=O bond), 1,068 and 979 (C–O and P–O bond, respectively).^{1}H NMR (400 MHz, δ in ppm, $CDCl_3$): 10.21 (br, 2H), 4.24 (br, 2H), 3.79 (br, 2H), 1.95 (s, 6H). ^{31}P NMR of δ in ppm (400 MHz, δ in ppm, $CDCl_3$):0.98.

Anchoring of ATRP—Initiator to MNs

To 10 mmol of ATRP-Initiator, (c), 10 mL of THF was added followed by the addition of 1-g magnetite nanoparticle. The mixture was sonicated for 24 h. The magnetite nanoparticle was separated using a bar magnet placed below the container and then rinsed with chloroform several times and finally with ethanol. It was dried under vacuum to get phosphonic immobilized magnetite-ATRP initiator, (d).

Surface Initiated ATRP of MMA from Magnetite Surface

The polymerization was carried out as follows: CuBr (0.070 mmol) and 50 mg of magnetite-ATRP initiator, (d), were added to a dry Schlenk flask with magnetic stirrer and rubber septum. It was degassed using vacuum line. This was followed by the addition of the degassed methyl methacrylate (27.86 mmol) (50 v/v of anisole). Then, the flask was charged with the pentamethyldiethyltriamine ligand (0.070 mmol) sealed under argon atmosphere, and was stirred in an oil bath maintained at 30 °C. After the desired time, the polymerization was stopped by opening the septum and diluting the reaction mixture with THF, followed by precipitation in 200 mL of hexane. Then the material was redispersed in ~5 mL of THF and centrifuged to remove homopolymer to obtain the hybrid material, (e), which was subjected to DRIFT-IR, TGA, XPS and GPC analyses.

Characterization

JASCO FTIR 410 (Japan) infrared spectrometer was used for recording DRIFT-IR spectra. The sample used here well ground with KBr. For neat IR spectra a thin film of polymer was cast on the CsCl disc from a dilute solution of polymer in THF. A Bruker 400 (400 MHz for proton) NMR spectrometer was used to record ^{1}H and ^{13}C spectra and $CDCl_3$ was used as the solvent. Molecular weights and molecular weight distributions of the degrafted polymer were determined by GPC measurements. GPC were performed at room temperature on a Waters GPC system with Waters 515 HPLC pump, three phenomenox columns in series (guard column, 500, 10^3, and 10^4 Å; 5-μm particle size), Waters 2487 dual λ absorbance UV detector and 2414 RI detector with Empower software data analysis package supplied by Waters (USA). THF was used as a solvent at a flow rate of 1 mL/min. Narrow molecular weight polystyrene standards were used for calibrating the GPC. The surface area was measured using BET (Brunauer-Emmett-Teller) adsorption isotherms method. Thermal analysis was performed using a Mettler Toledo STAR^{e} (Switzerland) thermal analysis system between ambient and 800 °C, at a heating rate of 20 °C/min under flowing nitrogen atmosphere (50 mL/min). The chemical composition of magnetite nanoparticle and polymer grafted magnetite nanoparticle were determined on a Physical Electronics 5600 spectrometer equipped with a concentric hemispherical analyzer of X-ray photoelectron spectroscopy (XPS), using an Al K_α X-ray source (15 KeV, filament current 20 mA) and the investigation of the sample was done under ultrahigh vacuum conditions of 10^{-9}–10^{-8} mbar with the takeoff angle being 45°. Transmission electron microscopy was carried out with a JEOL100CX transmission electron microscope applying an acceleration voltage of 100 kV. Samples were prepared by applying a drop of the particle solution in THF to a carbon-coated copper grid and imaged after drying.

Results and Discussions

Magnetite nanoparticles were prepared according to reported method [27] by adding 1:2 ratio of Fe^{+2}/Fe^{+3} to an aqueous solution, maintained in an inert atmosphere at a high pH which was obtained by addition of ammonia at ambient temperature. The powder XRD of MNs is shown

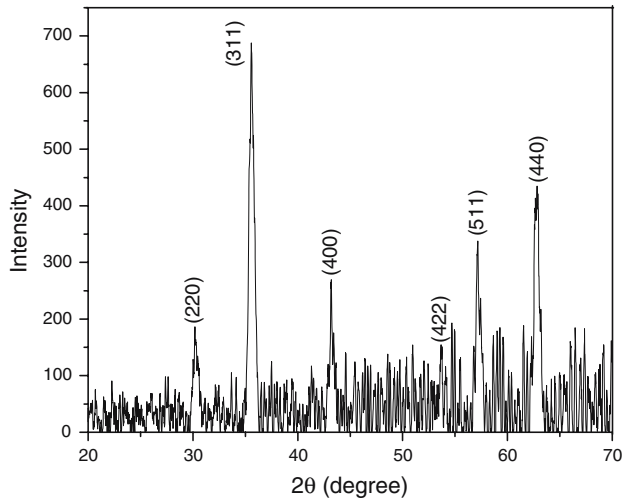

Fig. 1 The X-ray diffraction pattern of Fe_3O_4 nanoparticle (average size 13 nm)

Table 1 Atomic spacing observed for MNs as synthesized and the standard atomic spacing for Fe_3O_4 along with their respective hkl indexes from the PDF database

Sl. no.	1	2	3	4	5	6
d-value	2.96	2.52	2.10	1.70	1.61	1.48
Fe_3O_4	2.97	2.53	2.10	1.71	1.62	1.48
(hkl)	220	311	400	422	511	440

in Fig. 1. The reflection peak positions and relative intensities of the Fe_3O_4 nanoparticles, as synthesized, are shown in Table 1. These agree well with the standard XRD pattern of Fe_3O_4 nanoparticles [28], thus confirming the structure. The size of the Fe_3O_4 nanoparticle was deduced to be 13 nm from the peak width at half maximum (from 311 reflection) and Sherrer's formula. The surface area was measured by the BET method and is found to be 115 m^2/g. The X-ray photoelectron survey spectrum of the MNs is shown in Fig. 3a. This shows the characteristic doublet around 700 eV corresponding to Fe2p, and coincides with the value reported for MNs [29]. The atomic composition of the MNs indicates that its surface is predominately made of adventitious carbon to the extent of 61.25% (Table 2). The DRIFT-IR of the MNs is shown in Fig. 4a. MNs exhibit a strong band due to stretching mode of the –OH group at 3,400 cm^{-1}. Further the peak at 540 cm^{-1} corresponds to the inherent characteristic of the MNs [30].

The procedure followed for the synthesis of the initiator and covalent anchoring is described in Fig. 2. Initially 2-bromoisobutyrl bromide is reacted with anhydrous ethylene glycol, (a), at 0 °C to give the corresponding glycol bromoester, (b), which is suitably characterized by ^1H NMR and FTIR. The results are presented in the synthesis section. The ratio of the integrated areas under the methyl,

Table 2 Surface atomic composition of magnetite nanoparticles as determined by high resolution XPS, at a take off angle of 45°

Element	Magnetite	Magnetite with a monolayer of a ATRP initiator	Magnetite with a monolayer PMMA
C1s	61.3	40.6	63.5
O1s	34.2	43.5	32.0
P2p	–	1.3	0.8
Fe2p	4.3	13.7	2.0
Br3d	–	0.9	0.4

methylene and hydroxyl protons is seen to be 6:4:1 thus confirming the expected structure. The ATRP initiator and anchor molecule, (c), is obtained in the subsequent step involving the reaction of (b) with phosphorous oxychloride followed by hydrolysis. It was also characterized by ^1H NMR and ^{31}P NMR. The initiator was anchored to MNs by sonication. The XPS of the initiator-anchored MNs, (d), is shown in Fig. 3b and its atomic composition is presented in Table 2. For a monolayer of the initiator without any contribution from the underlying magnetite (Fe_3O_4) the expected values are: C = 42.9; O = 42.9; P = 7.1 and Br = 7.1. The atomic composition from XPS analysis is known to be sensitive to a surface depth of 3λ, where λ is the mean free path of the electron ($\lambda = 14$ Å for C_{1s} electron). The monolayer thickness is expected to be 8 ± 1 Å (based on bond angle and bond length), and hence signals from the underlying Fe and O atoms are seen in XPS analysis. Based on the atomic composition of Fe, P and Br of magnetite and for the monolayer it could be estimated that about 60% of the adventitious carbon (and oxygen) present on the "as synthesized" MNs has been displaced by the phosphonic acid monolayer. The peak at 72 eV corresponding to bromine [3d] atom confirms the anchoring of the initiator on the MNs surface. The increase in Fe_{2p} concentration from 4.31 for MNs (as synthesized) to 13.68%, suggests that a fraction of magnetite surface covered with adventitious carbon has been displaced. The DRIFT-IR of MNs anchored initiator is shown in Fig. 4b. The peaks at 1,724, 1,275, 1,009 cm^{-1} correspond to the carbonyl group of the bromo ester, the phosphonates P=O bond, and the P–O bond, while the peak at 543 cm^{-1} is characteristic of the MNs.

The bromine-terminated MNs were used to initiate the polymerization of methyl methacrylate, at ambient temperature, in the presence of CuBr/PMDETA complex, as described in Fig. 2. The polymerization was carried out successfully without the addition of sacrificial initiator. The use of sacrificial initiator would result in the formation of free polymer in solution, which has a tendency to physisorb to the MNs and in addition will have to be separated before use. To find the molecular weight and polydispersity

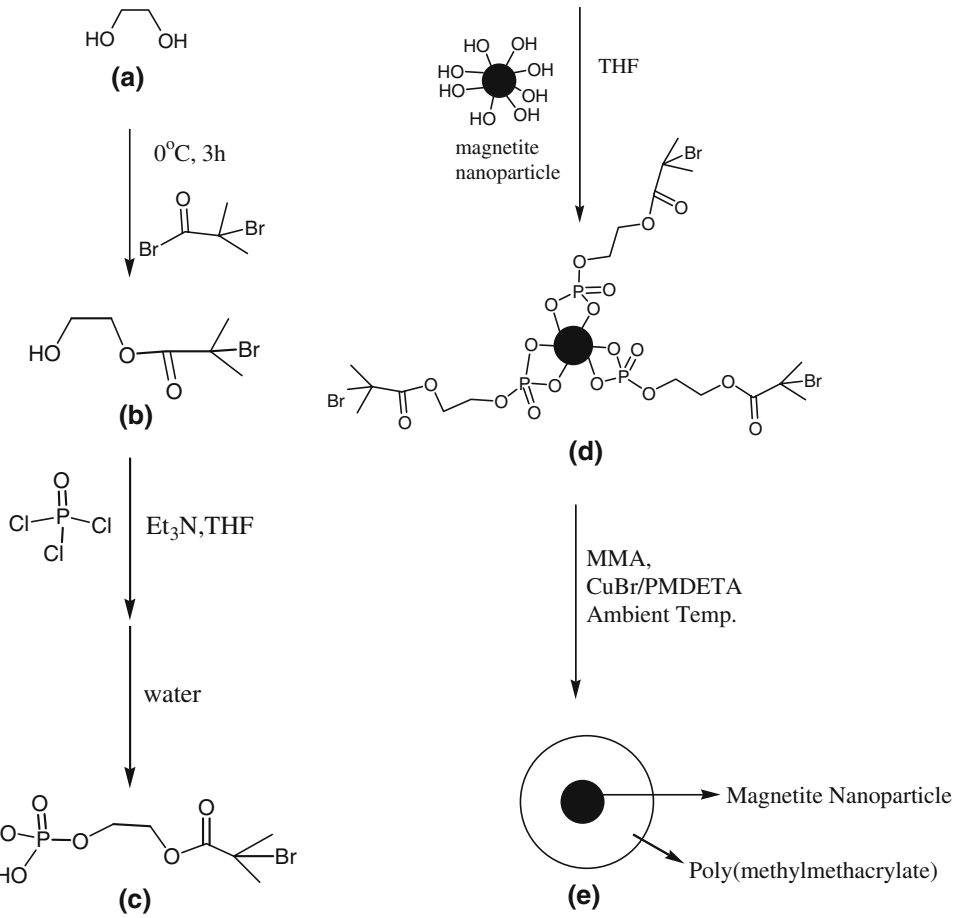

Fig. 2 Scheme for synthesis ATRP initiator and anchoring on magnetite nanoparticle

(M_n and M_w/M_n) of the grafted PMMA, the hybrid material was subjected to degrafting by using concentrated HCl in the presence of THF (mixture was allowed to stir overnight to obtain free polymer) followed by precipitation and drying. Following this the molecular weight (M_n) and polydispersity index (M_w/M_n) values of PMMA was measured by GPC. The results from this study are listed in Table 3. This shows that molecular weight of the polymer increases with the increase in the reaction time. However the polydispersity indices are greater than 2. This is due to the fact that a very low concentration of Cu (II), the persistent radical in ATRP, is generated during the surface polymerization (which in turn is due to the low concentration of the surface-initiating groups). It has been established that Cu (II) generated in the atom transfer equilibrium is vital in controlling the polymerization. Although the use of sacrificial initiator would alleviate this problem, by way of generating sufficient concentration of Cu(II) to control the atom transfer equilibrium, this would result in the formation of free polymer that will have to be separated from the reaction mixture.

The X-ray photoelectron survey spectrum of the MNs' surface after the grafting of poly(methylmethacrylate) brushes is shown in Fig. 3c. This is consistent with what would be expected of a monolayer of PMMA. The atomic composition (Table 2) also suggests that the polymerization had

Table 3 Results from the GPC analysis of degrafted PMMA M_nth = $([M]_o/[I]_o)(M_w$ of Methyl methacrylate)(conversion)/100 = 1.5×10^5 (g/mol)

Sl. no	Time (h)	$M_n \times 10^3$ (g/mol)	PDI	% weight loss[a]	Grafting density[b]	Initiator efficiency
1	3	17.6	2.46	75	0.85	0.43
2	6	27	2.39	80	0.74	0.40
3	9	32	2.36	87	1.07	0.55
4	12	42	1.94	88	0.89	0.45
5	15	50	2.00	90	0.92	0.47

[a] Determined by thermogravimetric analysis

[b] Grafting density calculated using Eq. 1 in chains/nm^2

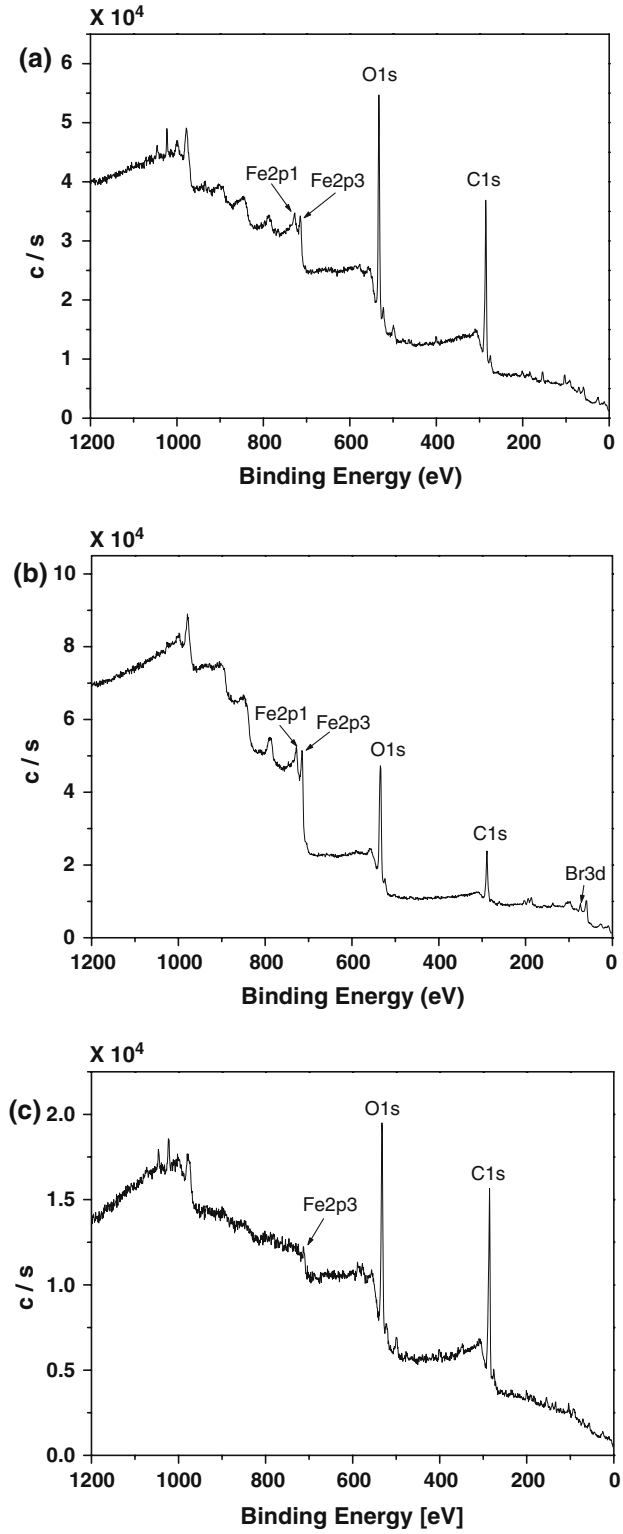

Fig. 3 X-ray photoelectron spectrum of (**a**) magnetite nanoparticle, (**b**) ATRP initiator anchored magnetite nanoparticle and (**c**) poly (methyl methacrylate) grafted magnetite nanoparticle

proceeded successfully from the surface-anchored ATRP initiator (obtained—C = 63.47 and O = 31.96, while expected values are 71.4 and 28.6, respectively). However

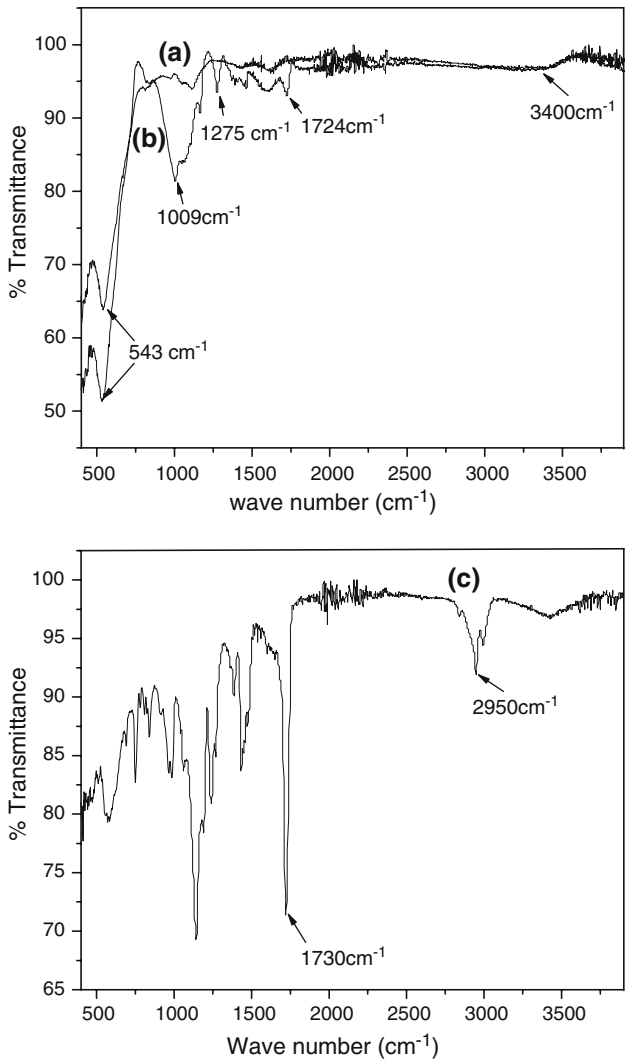

Fig. 4 RIFT-IR spectrum of (**a**) magnetite nanoparticle, (**b**) ATRP initiator-anchored magnetite nanoparticle and (**c**) poly(methyl methacrylate)-grafted magnetic nanoparticle

the XPS shows the presence of 2.01% of Fe and 0.8% P and this implies that the polymerization may not have taken place from some of the particles, which could be due to inadequate dispersion during the polymerization. The drift spectrum of PMMA-grafted MNs is shown in Fig. 4c. This shows an intense band at 1,730 cm^{-1} corresponding to the carbonyl group of poly(methyl methacrylate) along with C–H asymmetric stretching at 2,950 cm^{-1}.

Determination of Grafting Density for Initiator Efficiency

The PMMA-grafted MNs were subjected to thermogravimetric analysis. The result from the thermogravimetric analysis of MNs is shown in Fig. 5a. The initial weight loss observed, in the vicinity of 100 °C, is due to the continued loss of water [15]. The MNs were analysed by

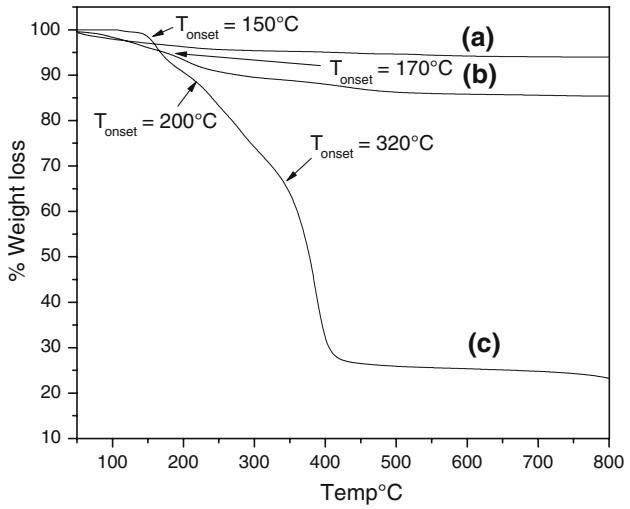

Fig. 5 Thermogravimetric analysis of (**a**) magnetite nanoparticle, (**b**) ATRP initiator anchored magnetite nanoparticle and (**c**) poly(methyl methacrylate)-grafted magnetite nanoparticle

thermogravimetric analysis following the anchoring of the ATRP initiator the result of which is shown in Fig. 5b. The weight loss at around 170 °C (T_{onset}) corresponds to the ATRP-initiator anchored on MNs. The graft density, δ, of the immobilized initiator molecules on MNs was calculated using the following Eq. 1 from the thermogravimetric analysis [31]. It was found to be 1.96 molecules/nm^2. The graft density can also be calculated from the XPS data [31] (Table 2) using Eq. 2, from the weight percentage of phosphorous defined as P in Eq. 2. The value of δ in this case is found to be 2.45 chains/nm^2. For comparison, the δ, value obtained on titania nanoparticles surface using hydrido-silane [32] anchoring chemistry is reported to be $\sim$1 chain/nm^2. Thus phosphonic acid group based anchoring could be a better alternative to hydridosilane and chlorosilane anchoring chemistries.

shown in Fig. 5c. The first weight-loss at 150 °C can be assigned to the decomposition of initiator moiety on the surface of magnetite. The subsequent rapid weight decrease in the second region (the onset at $\sim$200 °C) and the significant weight reduction in the third region (the onset at $\sim$300 °C) are attributed to the decomposition of PMMA. The grafting density as calculated from the TGA data is found to be nearly a constant value of $\sim$0.90 molecules/nm^2, throughout the polymerization time. Such constant grafting density throughout the polymerization time is typical of ATRP, as reported in the case of polymerization of MMA from silica nanoparticles at 70 °C [33]. The graft density is half of the value expected from the initiator graft density. This might be due to a very simple reason such as non-participation of some of MNs in the polymerization due to insufficient dispersion of the particles. It can also be accounted for by the fact that more radical–radical coupling followed by associated termination is likely to occur under surface polymerization conditions than conventional solution ATRP [25] of the same monomer, due to proximity of the propagating chain ends to each other. Thus to suppress this termination, normally sacrificial initiator is used so that sufficient concentration of Cu(II) is generated. However this results in the production of free polymer chains in solution. To avoid this as well as to minimize termination, a dilute system involving anisole as the medium was used to minimize the radical–radical coupling at adjacent sites. The reduction of initiator efficiency due to termination reaction between polymer chains growing in solution from free initiator and polymer chains growing from the surface resulting in the reduction of the initiator efficiency to 50% on silica nanoparticles via NMP has been reported [31].

The MNs were suspended in chloroform before and after the grafting of the PMMA brush to study the effect on their dispersion. The photographs of MNs, MNs with the

$$\text{Grafting density}\left(\mu\text{mol}/\text{m}^2\right) = \left[\{W_{60-730\,^\circ\text{C}}/100 - W_{60-730\,^\circ\text{C}}\}100 - W_{\text{magnetic}}/M\,S\,100\right]10^6, \quad (1)$$

$$\text{Grafting density}\left(\mu\text{mol}/\text{m}^2\right) = \left[10^6 P/\{3100 - P(M-1)S\}\right] \quad (2)$$

$W_{60-730\,^\circ\text{C}}$ is the weight loss in percentage of immobilized molecules on MNs after grafting, $W_{\text{magnetite}}$ is the weight loss in percentage for MNs before grafting, M is molar mass of the immobilized molecules on magnetite and S is the surface area of MNs.

For the polymer-grafted MNs, three main weight-loss regions are observed in thermogravimetric analysis, as

initiator, and with the PMMA brush are shown in Fig. 6a. The picture on the left is due to MNs as synthesized. This settles down rather quickly. The second picture from the left is due to MNs with the initiator anchored to the surface. It can be seen that the introduction of the initiator monolayer does seem to confer some dispersive stability. The third picture from the left is after the grafting of PMMA to MNs. It can be seen that a good dispersion is formed as a result of the growth of polymer chains from MNs surface. The photographs of MNs, MNs with the initiator and with the

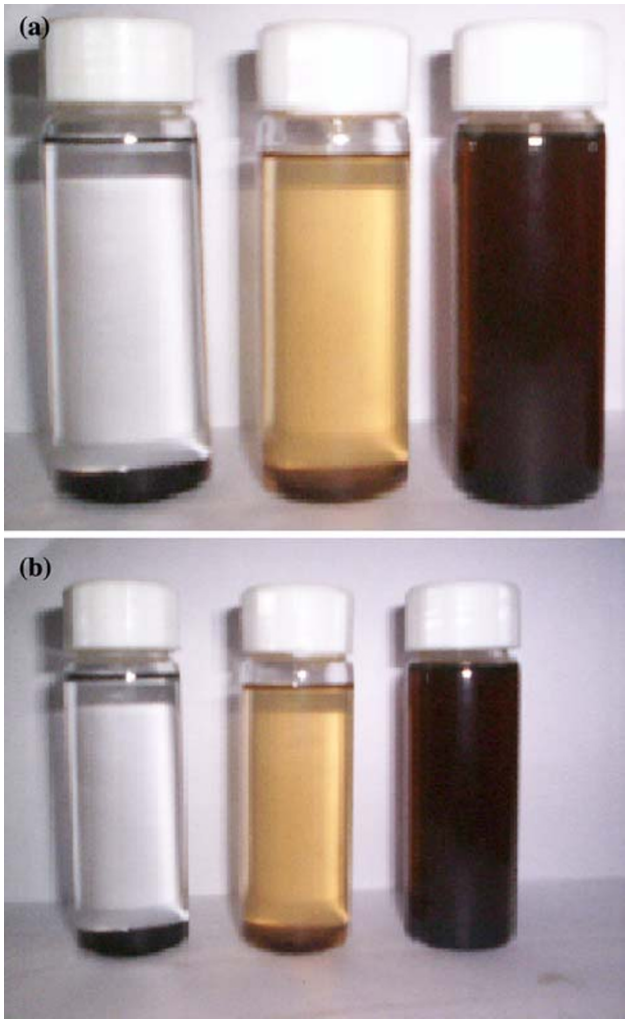

Fig. 6 Photographs (**a**) From the left of the photographs the magnetite particles and initiator grafted magnetite particles in chloroform settles down; polymer-modified magnetite particles form a stable dispersion and (**b**) stable dispersion of magnetite-polymer taken after 1 week

PMMA brush, after 1 week of observation time are shown in Fig. 6b. It can be seen that the PMMA brush does introduce reasonable long time stability to the dispersion of MNs, which is evident from the TEM studies as shown in Fig. 7b. The TEM image of unmodified magnetite nanoparticle is shown in Fig. 7a. This shows the formation of aggregates of about 200-nm size. Thus poly(methyl methacrylate) grafted on to the surface of MNs enables the dispersion of MNs in various organic solvents like THF, DCM and toluene.

Conclusion

A new molecule with phosphonic acid based anchor at one end and an ATRP initiator at the other end is synthesized and characterized. Due to the strong adsorption of phosphonic acid to a number of surfaces this molecule has wide

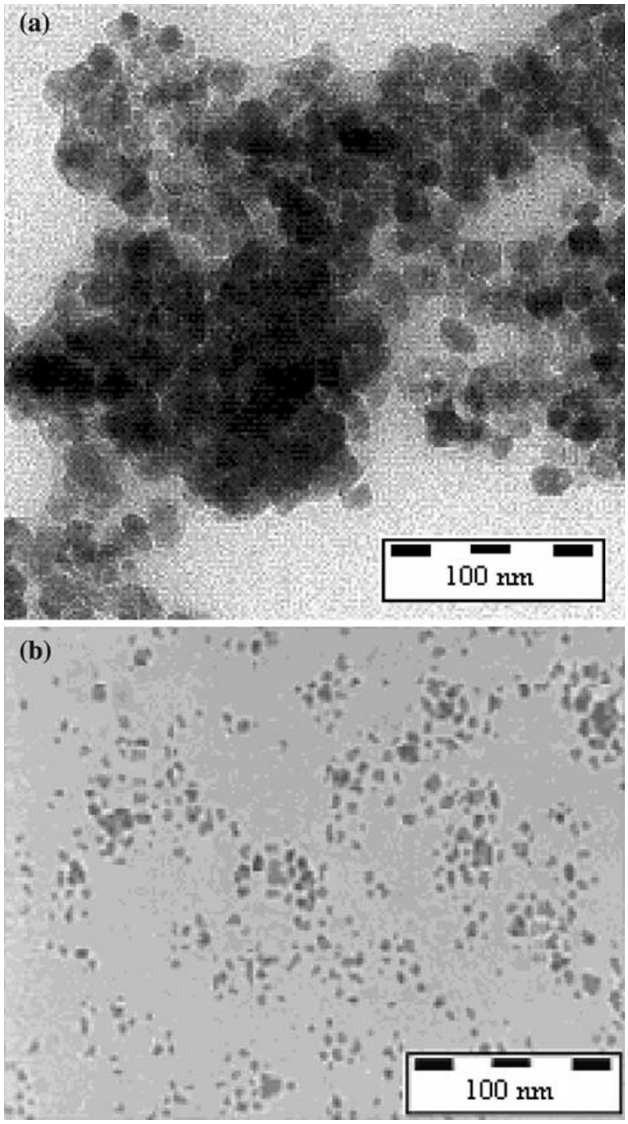

Fig. 7 TEM images of (**a**) unmodified magnetite nanoparticle and (**b**) magnetite–pmma hybrid material

applications towards extending ATRP from a variety of surfaces. The polymerization of MMA is initiated from the MNs surface to obtain poly(methyl methacrylate)-coated magnetite. The introduction of PMMA brushes on MNs provides enough dispersive stability as observed over a period of several months (data provided for 1-week sample only). This simple technique of synthesis and anchoring chemistry can be applied to various nanoparticles to produce polymer-stabilized nanoparticles.

References

1. M. Thakur, K. De, S. Giri, S. Si, A. Kotal, T.K. Mandal, J. Phys. Condens. Matter. **18**, 9093 (2006)
2. L.Y. Zhang, H.C. Gu, X.M. Wang, J. Magn. Magn. Mater. **311**, 228 (2007)

3. D.K. Kim, M. Mikhaylova, F.H. Wang, J. Kehr, B. Bjelke, Y. Zhang, T. Tsakalakos, M. Muhammed, Chem. Mater. **15**, 4343 (2003)
4. K.J. Tapan, M.A. Morales, S.K. Sahoo., D.L. Leslie-Pelecky, V. Labhasetwar, Mol. Pharm. **2**, 194 (2005)
5. X. Chenjie, K. Xu, H. Gu, R. Zheng, H. Liu, X. Zhang, Z. Guo, B. Xu, J. Am. Chem. Soc. **126**, 9938 (2004)
6. R.V. Christy, Z.J. Zhang, J. Am. Chem. Soc. **124**, 14312 (2002)
7. M. Ashok, H. Katz, P.M. Cotts, S. Subramoney, P. Mirau, J. Am. Chem. Soc. **127**, 14655 (2005)
8. I. Garcia, N.E. Zafeiropoulos, A. Janke, A. Tercjak, A. Eceiza, M. Stamm, I. Mondragon, J. Polym. Sci. Part A: Polym. Chem. **45**, 925 (2007)
9. M. Stephen, A.Y. Fadeev, Langmuir **20**, 2270 (2004)
10. A.E. Harrak, G. Carrot, J. Oberdisse, C.E. Baron, F. Boué, Macromolecules **37**, 6376 (2004)
11. R.M. Chicz, Z. Shi, F.E. Regnier, J. Chromatogr. **121**, 339 (1986)
12. A.B. Lowe, B.S. Sumerlin, M.S. Donovan, C.L. McCormick, J. Am. Chem. Soc. **124**, 11562 (2002)
13. O. Prucker, J. Rühe, Macromolecules **31**, 592 (1998)
14. M. Ryosuke, K. Yamamoto, H. Otsuka, A. Takahara, Chem. Mater. **15**, 3 (2003)
15. T. von Werne, T.E. Patten, J. Am. Chem. Soc. **123**, 7497 (2001)
16. C. Li, B.C. Benicewicz, Macromolecules **38**(14), 5929 (2005)
17. A.T. Christopher, J. Schwartz, Langmuir **23**(18), 9158 (2007)
18. P.H. Gregory, R. Sharma, J.O. Agola, S. Amin, V.C. Solomon, P. Singh, D.A. Buttry, J.L. Yarger, Chem. Mater. **19**, 2519 (2007)
19. R. Hofer, M. Textor, N.D. Spencer, Langmuir **17**, 4014 (2001)
20. J.M. Ferreira, S. Marcinko, R. Sheardy, A.Y. Fadeev, J. Colloid Interface Sci. **286**, 258 (2005)
21. E. Hoque, J.A. Derose. G. Kulik, P. Hoffmann, H.J. Mathieu, B. Bhushan, J. Phys. Chem. B. **110**, 10855 (2006)
22. T.J. Daou, S.B. Colin, J.M. Grenèche, F. Thomas, A. Derory, P. Bernhardt, P. Legaré, G. Pourroy, Chem. Mater. **19**, 4494 (2007)
23. R. Matsuno, K. Yamamoto, H. Otsuka, A. Takahara, Macromolecules **37**, 2203 (2004)
24. A. Ramakrishnan, R. Dhamodharan, J. Rühe, Macromol. Rapid Commun. **23**, 612 (2002)
25. K. Matyjaszewski, J. Xia, Chem. Rev. **101**, 2921 (2001)
26. M.A. White, J.A. Johnson, J.T. Koberstein, J. Turro, J. Am. Chem. Soc. **128**, 11356 (2006)
27. A. Miguel, C. Duarte, M. Giersig, N.A. Kotov, L.M. Liz-Marzán, Langmuir **14**, 6430 (1998)
28. T. Yang, C. Shen, Z. Li, H. Zhang, C. Xiao, S. Chen, Z. Xu, D. Shi, J. Li, H. Gao, J. Phys. Chem. B **109**, 23233 (2005)
29. S. Lian, Z. Kang, E. Wang, M. Jiang, C. Hu, L. Xu, Solid State Commun. **127**, 605 (2003)
30. I.J. Bruce, J. Taylor, M. Todd, M.J. Davies, E. Borioni, C. Sangregorio, T. Sen, J. Magn. Magn. Mater. **284**, 145 (2004)
31. C. Bartholome, E. Beyou, E.B. Lami, P. Chaumont, F. Lefebvre, N. Zydowicz, Macromolecules **38**, 1099 (2005)
32. G.K. Raghuraman, J. Ruhe, R. Dhamodharan, J. Nanopart. Res., doi: 10.1007/s 11051-007-9268-9 (2007)
33. K. Ohno, T. Morinaga, K. Koh, Y. Tsujii, T. Fukuda, Macromolecules **38**, 2137 (2005)